Optimization of the gain in non-uniform gratings in a Bi$_{12}$SiO$_{20}$ crystal considering the variation of fringe period, optical activity and polarization angles in a strong non-linear regime

G. González and A. Zúñiga
Escuela Superior de Física y Matemáticas, Instituto Politécnico Nacional,
Edificio 9, Unidad profesional Adolfo López Mateos, 07730, México D.F., México.

L.F. Magaña*
Instituto de Física, Universidad Nacional Autónoma de México,
Apartado Postal 20-364, México, 0100 Distrito Federal.

We solved numerically the set of non-linear differential material rate differential equations, and using these solutions, we include the non-uniformity of the grating and of the magnitude and phase of light modulation along a sample thickness to calculate self-consistently the energy exchange in two-wave mixing. We optimize the gain, considering strong nonlinear conditions, variation of fringe period, optical activity, birefringence, absorption, polarization angle, applied fields and two crystal orientations: the grating vector parallel and perpendicular to the face [001] Under these conditions there is a complex relationship among all these parameters, and the prediction of the conditions for the optimum value of the gain is not simple We report the optimal sample thickness for different situations We obtained a maximum gain of 5.2.

Keywords: Photorefractive gratings; refractive index; beam coupling; energy exchange; non-linear optics.

Resolvimos numéricamente el conjunto de ecuaciones diferenciales parciales no lineales del material y, usando estas soluciones, incluimos la no uniformidad de la rejilla y de la magnitud y de fase de la modulación de la luz a lo largo del espesor de la muestra para calcular auto consistentemente el intercambio de energía del mezclado de dos ondas. Optimizamos la ganancia considerando condiciones fuertemente no-lineales, la variación del tamaño de la rejilla, actividad óptica, birefringencia, absorción, ángulos de polarización, campos aplicados, y dos orientaciones cristalinas: el vector de la rejilla paralelo y perpendicular a la cara [001]. Bajo estas condiciones existe una relación compleja entre todos estos parámetros, y la predicción de las condiciones para el valor óptimo de la ganancia no es simple. Reportamos el espesor óptimo de la muestra para diferentes situaciones. Obtenemos una ganancia máxima de 5.2.

Descriptores: Acoplamiento de haz; intercambio de energía; óptica no lineal.

PACS: 42.65.-k; 42.70.-a; 42.70.Nq

1. Introduction

BSO (Bi$_{12}$SiO$_{20}$) is a photorefractive material of the sillenite family with a high response rate, high sensitivity, unlimited recyclability and large holographic storage times with a good potential technological use [1-3]. For thick samples with no very large absorption coefficient, under a non-linear regime, we have a strong beam coupling and there is a spatial redistribution of the light intensity pattern that changes the light modulation across the crystal. In this way the grating is spatially non-uniform and its amplitude and phase change within the sample along the sample thickness, z. It was shown recently that the non-uniformity of the grating is of great relevance to the energy exchange and to the influence of the input polarization angles on the gain [4].

When a large absorption coefficient is present, the light waves decay very rapidly inside the sample, and the energy exchange as well as the spatial non-uniformity of the grating become irrelevant. However, it is possible to obtain low absorption coefficients in sillenites with adequate doping [5,6].

In this work we considered a non-moving transmission grating We solved numerically the set of non-linear material rate differential equations. We used these solutions to study

the optimization of the gain including the non-uniformity of the grating and of the magnitude and phase of light modulation along a sample thickness, considering the variation of the fringe period. We studied thick BSO crystals where the effects of beam coupling become significant. We followed a vector approach [7-10] to express the two-wave coupling equations that represent the recording process, including optical activity, birefringence, absorption of light and several values of light modulation and polarization angles of the incident beams. We considered two optical configurations for K$_G$ (the grating vector) K$_G$ ∥ [001] and K$_G$ ⊥[001] for different values of d.c applied fields. The solutions to the corresponding two sets of beam coupling equations were obtained numerically in a self-consistent way.

2. Coupled wave equations

We took as intensity of the interference light pattern

$$I(x) = I_0(1 + |m(z)| \cos K_G x), \qquad (1)$$

where I is the total intensity of the light and $m(z)$ is the light modulation which varies along the sample thickness accord-

ing to:

$$m(z) = 2\frac{[A_{1\xi}(z)A_{2\xi}(z)^* + A_{1\varsigma}(z)^*A_{2\varsigma}(z)]}{I_0} \quad (2)$$

Where we considered the interaction of two plane, monochromatic, linearly polarized electromagnetic waves, $\vec{A}_1(z)$ and $\vec{A}_2(z)$, that propagate inside the sample. Each field has two components: one, along $\hat{u}_\varsigma$ perpendicular to the plane of incidence $(x - z)$ and the other, along $\hat{u}_\xi$ parallel to the same plane. The total light field can then be written as the superposition of the two:

$$\vec{A}(\vec{r}) = \vec{A}_1(z)\exp(-i\vec{k}_1 \bullet \vec{r}) + \vec{A}_2(z)\exp(-i\vec{k}_2 \bullet \vec{r}_2), \quad (3)$$

where $\vec{k}_1$ and $\vec{k}_2$ are the corresponding wave vectors, and

$$\vec{A}_1(z) = A_{1\xi}(z)\hat{u}_\xi + A_{1\varsigma}(z)\hat{u}_\varsigma; \;\; \vec{A}_2(z) = A_{2\xi}(z)\hat{u}_\xi + A_{2\varsigma}(z)\hat{u}_\varsigma$$

With this interference pattern in the photorefractive material the light excites electrons to the conduction band, which migrate due to diffusion and drift from the bright to the dark parts of the crystal where they are captured by the compensating centers, resulting in the appearance of a space charge field. These phenomena are described with the usual one-trap-one band model [1112] by the following set of equations:

$$\frac{\partial N^+}{\partial t} = (sI + \beta)(N - N^+) - \gamma nN^+ \quad (4)$$

$$\frac{\partial n}{\partial t} = \frac{\partial N^+}{\partial t} - \frac{\nabla \cdot j}{e} \quad (5)$$

$$j = e\mu nE - eD\nabla n + pI \quad (6)$$

$$\frac{\partial(\varepsilon\varepsilon_0 E)}{\partial x} = e(n + N_A - N^+) \quad (7)$$

The motion of the carriers, of charge e, is along the x coordinate, N_A is the initial number of acceptors or compensating centers, N^+ is the concentration of ionized donors at instant t and N^+ is the total concentration of donors. The current density is j, the electron concentration is n and their mobility μ, D is the diffusion coefficient, γ the trapping coefficient, β the thermal ionization rate, s the photo ionization cross section, ε the dielectric constant, pI the photovoltaic current, p the photovoltaic constant (effective Glass coefficient) and ε_0 the permittivity in free space. The total electric field is E, which is given by the sum of E_a (external d.c. field) and the induced space charged field $E_{esc.}$

We solved numerically the set of non-linear material rate differential equations (4) for several values of fringe spacing, Λ : 1, 2, 3, 4, 5, 7, and 10 microns. In this manner we obtained the variation of the overall space charge field as a function of light modulation for each value of the applied field (5 and 10 Kv/cm) We followed the method described elsewhere [13]. For each one of these values of fringe spacing we obtained the numerical solutions for several values of m_0, the value of light modulation at the surface of the sample,

TABLE I. Parameters for BSO [7, 14, 16, 17] taken for our calculations.

BSO		
ε	Dielectric constant	56
n_0	Average refractive index	2.5
r	Electro optic coefficient (mV^{-1})	4.7×10^{-12}
N_D	Donor density (m^{-3})	10^{25}
N_A	Acceptor density (m^{-3})	10^{22}
μ_τ	Mobility lifetime product (cm^2 V^{-1})	1×10^{-7}
γ	Recombination constant (m^{3}s^{-1})	1.6×10^{-17}
s	Photo ionization cross section (m^{2}J^{-1})	1×10^{-5}
α	Absorption coefficient (cm^{-1}) $\lambda = 532$nm	0.65
ρ	Optical activity (°/cm) $\lambda = 532$nm	$386 \sim 6.74$ cm^{-1}

between 0 and 1. Then we performed the Fourier decomposition for each of the calculated overall space charge fields to obtain the amplitude, E_1 of its fundamental Fourier component and its phase, Φ which is the dephasage of the space charge field with regard to the light interference pattern, for every one of the cases considered. It is necessary to mention that this method does not rely on a Fourier expansion and so its validity is not limited by the use of a truncated harmonic basis. In this way we have obtained the grating strength and its phase as functions of light modulation which are necessary to solve self-consistently the beam coupling equations. The parameters used for the BSO are shown in Table I.

In this work we considered a crystal cut to expose the $(\bar{1}10)$, the (110) and the (001) crystallographic faces. To deal with the two wave mixing (TWM) problems, we followed a tensor approach, taking into account optical activity, birefringence, absorption of light, for the two common optical configurations, the first with $K_G \parallel [001]$ and the light waves are propagating in the $(\bar{1}10)$ plane. The second configuration is with $K_G \perp [001]$ where $K_G \parallel [\bar{1}10]$ and the light waves propagate in the (001) plane, and the applied electric field is parallel to K_G [7,8] For each configuration, the corresponding set of differential equations is obtained by the substitution of the light field, $\vec{A}(r)$ given, by Eq. (3), and the electric displacement tensor, $\vec{D}(r)$, in the steady state wave equation,

$$\nabla^2 \vec{A}(r) + \frac{k_0^2}{\varepsilon_0}\vec{D}(r) = 0 \quad (8)$$

$\vec{D}(r)$ in a sillenite medium can be expressed as

$$D_i = \varepsilon_0(\varepsilon_{ij} + G_{ij} + \Delta\varepsilon_{ij})E_j \quad (9)$$

where ε_{ij} is the symmetric optical permittivity tensor in the absence of optical activity and electro-optic coupling G_{ij} is the tensor describing the optical activity, E_j is the j component of the electric field, $\Delta\varepsilon_{ij}$ is the variation of the optical permittivity tensor induced by the linear Pockels electro-

optical effect. For simplicity we are neglecting the photo-voltaic and photo galvanic effects. The piezoelectric and photo elastic effects, for crystals of the sillenite family with the configurations we are considering can be neglected [8] The permittivity and the optical activity tensors are expressed in the light propagation coordinate system.

Finally, neglecting the second derivate of the field the following set of equations for K$_G$ ∥ [001] with the light waves propagating in the ($\bar{1}$ 10) plane is obtained [7,8]:

$$\frac{dA_{1\varsigma}(z)}{dz} = -\rho A_{1\xi}(z) - \frac{\alpha}{2} A_{1\varsigma}(z) \tag{10}$$

$$\frac{dA_{1\xi}(z)}{dz} = \rho A_{1\varsigma}(z) + i\kappa_0 A_{1\xi}(z) + i\kappa_1^*(z) A_{2\xi}(z)$$
$$- \frac{\alpha}{2} A_{1\xi}(z) \tag{11}$$

$$\frac{dA_{2\varsigma}(z)}{dz} = -\rho A_{2\xi}(z) - \frac{\alpha}{2} A_{2\varsigma}(z) \tag{12}$$

$$\frac{dA_{2\xi}(z)}{dz} = \rho A_{2\varsigma}(z) + i\kappa_0 A_{2\xi}(z) + i\kappa_1(z) A_{1\xi}(z)$$
$$- \frac{\alpha}{2} A_{2\xi}(z) \tag{13}$$

Here α is the absorption coefficient and ρ is the optical activity. The constant κ, is due to the variation of the magnitude of the change in the refractive index induced by the external applied field, E:

$$\kappa_0 = \frac{2\pi \Delta n_0}{\lambda \cos\theta} \tag{14}$$

where

$$\Delta n_0 = \frac{n_0^3 r E_0}{2} \tag{15}$$

n is the average refraction index in the sample, λ is the wave length of the recording monochromatic beams, θ is the incidence Bragg's angle and r is the electro-optic coefficient. Notice that κ_0 is not a function of z.

The coupling factor, κ_1 is due to the space charge field obtained from the solution of the material rate equations; it is complex, and a function of z:

$$\kappa_1(z) = \frac{\pi \Delta n_1(z)}{\lambda \cos\theta} \tag{16}$$

where $\Delta n_1(z)$ is the modulated change of the refractive index induced by the space charge field through the linear electro-optic effect:

$$\Delta n_1(z) = n_o^3 r * \frac{|E_1(z)|}{2|m(z)|} * e^{i\Phi(z)} * m(z) \tag{17}$$

where Φ is the dephasage of the space charge field with regard to the light interference pattern, z being the coordinate along the sample thickness, which is in the same direction as the light beam propagation and $m(z)$ the complex light modulation, given by Eq. (3). $E_1(z)$ is the fundamental Fourier

component of the space charge field, and Eq. (16) can be written as:

$$\kappa_1(z) = \frac{\pi}{\lambda \cos\theta} \frac{n_0^3 r |E_1(z)|}{2} \exp i(\Phi(z) + \psi_m(z)) \tag{18}$$

here $\psi_m(z)$ is the phase of the light modulation

Notice that we are considering not only the magnitude of the variation of the refractive index along the sample thickness, but also the variation of its phase. It is important to take this into consideration when a static d.c. electric field is applied, because the phase Φ is no longer $\pi/2$ as in the diffusion regime. The phase in this case is a function of both the value of the applied field and the coordinate along the sample thickness

The corresponding set of coupled wave equations for K$_G$ ⊥ [001] and the light waves traveling in the (001) plane is [7,8]:

$$\frac{dA_{1\xi}(z)}{dz} = (\rho - i\kappa_0) A_{1\varsigma}(z) - i\kappa_1^*(z) A_{2\varsigma}(z)$$
$$- \frac{\alpha}{2} A_{1\xi}(z) \tag{19}$$

$$\frac{dA_{1\varsigma}(z)}{dz} = -(\rho + i\kappa_0) A_{1\xi}(z) - i\kappa_1^*(z) A_{2\xi}(z)$$
$$- \frac{\alpha}{2} A_{1\varsigma}(z) \tag{20}$$

$$\frac{dA_{2\varsigma}(z)}{dz} = -(\rho + i\kappa_0) A_{2\xi}(z) - i\kappa_1(z) A_{1\xi}(z)$$
$$- \frac{\alpha}{2} A_{2\varsigma}(z) \tag{21}$$

$$\frac{dA_{2\xi}(z)}{dz} = (\rho - i\kappa_0) A_{2\varsigma}(z) - i\kappa_1(z) A_{1\varsigma}(z)$$
$$- \frac{\alpha}{2} A_{2\xi}(z) \tag{22}$$

The solutions to each set of beam coupling equations (7) and (13) have to be self-consistent. This is because the changes in the intensities of waves and phases cause changes in the light modulation and in the refraction index and these, in turn, induces new changes in the intensity of the waves.

We solved each set of equations with no restrictions on the parameters (ρ, κ_o, κ_1). We divided the sample in thin layers of thickness Δz [14] in such a way that within each layer, $\kappa_1(z)$ is practically constant. In this way within each layer we have analytical solutions [4] for the coupled equations of sets (7) and (13). When a small change (larger than 0.1%) in this variable occurred, we chose a smaller interval and calculated the new corresponding set of values of constants for the corresponding interval Δz. We started evaluating the initial set of constants for the first layer at the surface of the sample by using $\kappa_1(z = 0)$. Next, for the following layers, the values of the complex amplitudes of the beams at the end of each interval were used to evaluate $m(z)$ and therefore a new value of κ_1 at z where the following layer starts. The analytical solutions for a constant, $\kappa_1(z)$ for the two sets of equations (7) and (13) for K$_G$ ∥ [001] and K$_G$ ⊥ [001] are given elsewhere [4].

We used gratings with different spatial periods Λ of 1, 2, 3, 4, 5, 7, and 10 microns light modulation at the surface of the sample (m) of 0.9, 0.6, 0.3 and 0.1. We applied two fields: 5.0 and 10.0 kV/cm The values of absorption and optical activity used for BSO crystals are given in Table I We also considered that the two beams were linearly polarized and had the same polarization angles at the surface of the sample. The polarization angle is ϕ_p, defined as the inclination angle of the electric field of light waves with respect to the plane of incidence at the surface of the sample,

$$\varphi_{pi} = \tan^{-1}\left[\frac{A_{i\xi}(z=0)}{A_{i\xi}(z=0))}\right], i = 1, 2 \qquad (23)$$

From the complex amplitudes of light waves, obtained from the self-consistent solutions of each set of equations, we calculated the intensities, phases of each wave and the corresponding light modulation $m(z)$ as a function of z. For each of the recording orientations we also obtained the two-wave gain, $\Gamma_{ij}(z)$ defined as:

$$\Gamma_{ij}(z) = \left(\frac{1}{z}\right)\ln\frac{I_i(z)I_j(0)}{I_i(0)I_j(z)}, i,j = 1,2; i \neq j \qquad (24)$$

This is related to the one-wave effective gain $G_k(z)$ defined by:

$$G_k(z) = \frac{I_k(z)}{I_k(0)} - 1; k = 1, 2 \qquad (25)$$

where $I_l(z) = |A_l(z)|^2$ is the intensity of the corresponding light beam l at the specific sample thickness z, and $I_l(z=0)$ is the intensity of this light beam at the surface of the sample.

Definitions (24) and (25) are related by:

$$\Gamma_{ij}(z) = \left(\frac{1}{z}\right)\ln\left|\frac{1+G_i(z)}{1+G_j(z)}\right|, i,j = 1,2; i \neq j \qquad (26)$$

It is clear that: $\Gamma_{ij}(z) = -\Gamma_{ji}$

3. Results and discussion

All our calculations were performed using an absorption coefficient, $\alpha = 0.65$ cm^{-1} and optical activity $\rho = 386°$ cm^1. In Fig. 1 we show the two-wave gain (Eq. (24)), as a function of the sample thickness, for four different values of grating spacing (1, 3, 4 and 10 microns) under an applied field of 5 Kv/cm, with $m = 0.1$ K$_G \parallel$ [001], and initial polarization angles, $\Phi_{p,}$ of 0, for the writing beams. Note that the value of the thickness for all fringe periods with the maximum magnitude of the gain, is around 2 mm. For this case it is interesting to notice that, for this sample thickness, the grating with the largest gain corresponds to a grating spacing of 1.0 microns, and the value of the maximum magnitude of the gain is around 1.5 cm^{-1}. For samples with a thickness larger than 1.0 cm, this same grating space becomes the one with the minimum magnitude of the gain.
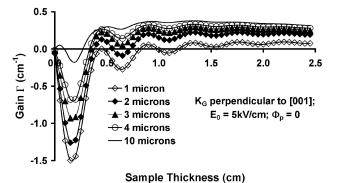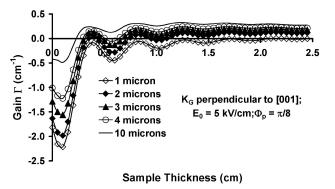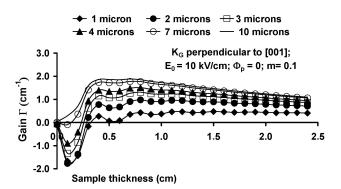

FIGURE 1. Results of the gain, along the sample thickness, for different values of BSO grating spacing recorded with an applied field of $E_0=5$ Kv/cm, $m_0 = 0.1$ for K$_G \perp$ [001] with absorption ($\alpha=0.65$) cm^{-1} optical activity ($\rho=386°$ cm^{-1}) and with initial polarization angles of 0 for the writing beams.

FIGURE 2. Results of the gain, along the sample thickness, for different values of BSO grating spacing recorded with an applied field of $E_0=5$ Kv/cm, $m_0 = 0.1$ for K$_G \perp$ [001], with absorption ($\alpha=0.65$) cm^{-1} optical activity ($\rho=386°$ cm^{-1}) and with initial polarization angles of for the writing beams of $\pi/8$.

FIGURE 3. Results of the gain, along the sample thickness, for different values of BSO grating spacing recorded with an applied field of $E_0 =10$ Kv/cm, $m_0 = 0.1$, for K$_G \perp$ [001], with absorption ($\alpha=0.65$)cm^{-1} optical activity ($\rho=386°$ cm^{-1}) and with initial polarization angles of 0 for the writing beams.
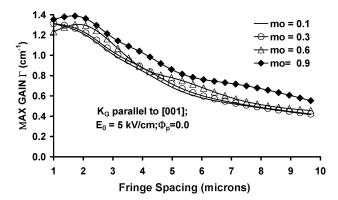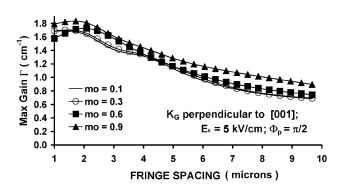
FIGURE 4. Results of the maximum gain, as a function of the BSO grating period, for different values of initial light modulation at the surface of the sample, m_0, recorded with an applied field of E_0 =5Kv/cm, for K$_G$ ∥ [001], with absorption (α=0.65) cm^{-1} optical activity (ρ=386° cm^{-1}) and with initial polarization angles of 0 for the writing beams.

FIGURE 5. Results of the maximum gain, as a function of the BSO grating period, for different values of initial light modulation at the surface of the sample, m_0 (0.1, 0.3, 0.6, 0.9), recorded with an applied field of E_0 =5Kv/cm, for K$_G$ ⊥ [001], with absorption (α=0.65) cm^{-1} optical activity (ρ=386° cm^{-1}) and with initial polarization angles of $\pi/2$ for the writing beams.
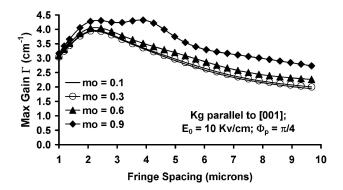

FIGURE 6. Results of the maximum value of the gain, as function of BSO grating spacing recorded with an applied field of E_0 =10 Kv/cm, for different values of m_0 (0.1, 0.3, 0.6, 0.9) for K$_G$ ∥ [001], with absorption (α=0.65) cm^{-1} optical activity (ρ=386° cm^{-1}) and with initial polarization angles of $\pi/4$ for the writing beams.

In Fig. 2, we show results for the same conditions as those of Fig. 1, but for $\Phi_p = \pi/8$. Now the value of optimal sample thickness, (the thickness required for the maximum magnitude of the gain) is around 1mm, which is a bit smaller than the corresponding one in Fig. 1 and the maximum magnitude of the gain is a bit larger (2.2 cm^{-1}) that the corresponding one in Fig. 1. Notice that the value of the gain for $z = 0$ is not zero. This can be easily understood using a Taylor expansion in Eq. (24). We have that for $z \approx 0$ it is straightforward to obtain:

$$\Gamma_{ij}(z \approx 0) \approx \left(\frac{d}{dz} \left[\ln \left(\frac{I_i(z)}{I_j(z)} \right) \right] \right)_{z=0}$$

It is clear that $\Gamma_{ij}(z = 0)$ may be different from zero.

Conditions for Fig. 3 are the same as in Fig. 1, but with an applied electric field, E_0, of 10 kV/cm. We can see that the increase in the applied electric field implied an increment of the magnitude of the gain from 1.5 to 1.9. However, this increment is smaller than that obtained by changing the polarization angle of the recording beams as shown in Fig. 2. Notice that, for a thickness larger that 5 mm, the largest value of the gain is for the grating with the largest period.

In Figs. 4 to 7 we show results for the maximum magnitude of the gain as a function of grating period for several values of the light polarization at the surface of the sample. In Fig. 4 we have E_0=5 kV/cm, K$_G$ ∥ [001] and $\Phi_p = 0$ for the writing beams The maximum magnitude of the gain is 1.4 cm^{-1} and corresponds to a grating period of 2 microns, with $m = 0.9$, and the gain, for all values of m decreases by a factor of around 3.5 when the grating period goes from 2 to 10 microns.

For Fig. 5 we have E_0=5 kV/cm K$_G$ ⊥ [001], and $\Phi_p=\pi/2$. The maximum magnitude of the gain is 1.8 cm^{-1}, for a fringe spacing of 2 microns, with $m = 0.9$ and the gain in all cases decreases as fringe spacing increases. $m = 0.9$ The gain values for fringe spacing between 1 and 5 microns are very similar.

In Fig. 6 we have E_0=10 kV/cm K$_G$ ∥ [001], and $\Phi_p = \pi/4$. The maximum magnitude of the gain is around 4.5 cm^{-1}, and it happens for m= 0.9. The gain values are very similar for all values of m for fringe spacing between 1 and 2 microns. The largest maximum magnitude of the gain remains approximately constant for fringe spacing between 2 and 4 microns and $m = 0.9$ Again, the maximum magnitude of the gain in all cases decreases as fringe spacing increases. With the exception of the case $m = 0.9$,the values of the maximum magnitude of the gain are very similar for all values of fringe spacing.

In Fig. 7 we have E_0=10 kV/cm K$_G$ ∥ [001], and $\Phi_p = \pi/2$. The maximum magnitude of the gain is around 5.2 cm^{-1}. Again with the exception of the case $m = 0.9$, the values of the maximum magnitude of the gain are very similar for all values of fringe spacing, and the largest values correspond to the case $m = 0.9$. However, for fringe spacing between 1 and 2 microns the results are very similar in all cases.
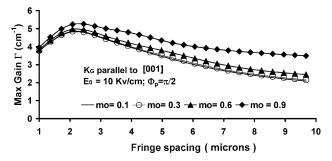
FIGURE 7. Results of the maximum value of the gain, as a function of the grating spacing recorded with an applied field of E_0=10 kV/cm, for different values of m_0 (0.1, 0.3, 0.6, 0.9) for $K_G \parallel$ [001], with absorption (α=0.65) cm^{-1} optical activity (ρ=386° cm^{-1}) and with initial polarization angles of $\pi/2$ for the writing beams.
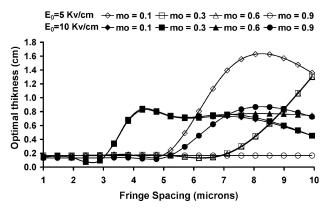

FIGURE 8. Optimal values for sample thickness to get the maximum value of the magnitude for the gain, as a function of the grating spacing, when $K_G \perp$ [001] and the initial polarization angle of the incident beams is 0, for two values of the applied field: 10 kV/cm and 5 kV/cm. We show results for different values of the initial light polarization: m_0= 0.1, 0.3, 0.6 and 0.9.

Figure 8 shows the optimal sample thickness as function of fringe spacing to get the maximum magnitude of the gain with $K_G \perp$ [001], and $\Phi_p = 0$, for two possible values of the applied field: E_0=10 kV/cm and E_0=5 kV/cm We mention some relevant features. Notice that for fringe spacing below 3 microns the optimal thickness is, for all cases, around 2mm. For fringe spacing between 3 and 5 microns, this value for the optimal thickness remains the same except for the case $m = 0.3$ with $E = 10$ kV/cm, which has an optimal thickness of 8 mm. We can see the largest optimal thickness in this figure is around 1.6 cm for $m = 0.1$ and $E = 5$ kV/cm and it is for a fringe spacing of 8 microns. If E =10 kV/cm the largest optimal thickness is 8.3 mm for $m = 0.3$ and m= 0.6 when the fringe spacing is around 4 microns, and remains nearly

constant up to 10 microns; for $m = 0.9$, the largest optimal thickness is around 8 mm for a fringe spacing of 8 microns.

It is necessary to mention that, as pointed out in Ref. 15 the gain changes its magnitude when a sample rotation of 180° is made around the direction of propagation of the light waves (our z axis). In this case there is a change in sign of the electro-optic coefficient and a weakening of the weak beam occurs instead of a weakening of the strong beam [15].

4. Conclusions

We studied, under strong non-linear conditions the optimization of the gain during two-wave mixing in non-uniform gratings in BSO for thick samples with a small absorption coefficient. From the results of our self-consistent calculation, we have exhibited how this optimization can be obtained Given a BSO sample (with a fixed absorption coefficient and a fixed value for optical activity), we have to combine adequately sample orientation, fringe spacing initial light modulation, optical activity, initial polarization angles, applied electric fields and sample thickness. There is a complex relationship among all these parameters, and the prediction of the conditions for the optimum value of the gain is not simple We can see cases where, with an applied field of 5 Kv/cm (see Fig. 3), we obtain for the magnitude of the gain, values larger than the corresponding ones obtained with an applied field of 10 Kv/cm (see Fig. 3). From our results it is clear that an adequate combination of sample thickness, sample orientation, polarization angle of the incident beams and fringe spacing can be more important for reaching a larger value for the magnitude of the gain, than increasing the applied field. It is convenient to stress that for a given set of these parameters, if the electric field is increased, the gain will increase. The maximum gain we obtained is around 5.2 for a fringe spacing of 2 microns, $K_G \perp$ [001], applied field of 10 Kv/cm, light modulation at the surface of the sample of 0.9, and initial polarization angle of the incident beams of $\pi/2$, with a sample thickness of 0.3mm. On the other hand, we found for the maximal amplification factor a value of 5.8 for $K_G \parallel$ [001]. Applied field = 10 kV/cm, Φ_p= $\pi/2$, and $m_0 = 0.1$, for a thickness of 1.9 cm, and a grating period of 2 microns.

Acknowledgements

∗. Author to whom correspondence should be addressed: Tel. + [52 55] 56 22 51 22; FAX + [52 55] 56 22 50 11; e-mail: fernando@fisica.unam.mx

1. P. Gunter and J.P. Huignard, *Photo Refractive Materials and their Applications, vol. I* (Springer-Verlag, Berlin, 1988); P. Gunter and J.P. Huignard, *Photo Refractive Materials and their*

Applications, vol. II (Springer-Verlag, Berlin, 1989).

2. P. Buchhave, S. Lyuksyutov, M. Vasnetsov, and C. Heyde, *J. Opt. Soc. Am. B* **13** (1996) 2595.

3. S.F. Lyuksyutov, P. Buchhave, and M.V. Vasnetsov, *Phys. Rev. Lett.* **79** (1997) 67.

4. L.F. Magaña, I. Casar, and J.G. Murillo, *Opt. Mater.* **30** (2008) 979.

5. S.L. Hou, R.B. Laurer, and R.E. Aldrich, *J. Appl. Phys.* **44** (1973) 2652.

6. I. Foldvari, L.E. Halliburton. and G.J. Edwards, *Sol. Stat. Com.* **77** (1991) 181.

7. A. Marrakchi, R.V. Johnson, and J.A.R. Tanguay, *J. Opt. Soc. Am. B* **3** (1986) 321.

8. V.V. Shepelevich, N.N. Egorov, and V. Shepelevich, *J. Opt. Soc. Am. B* **11** (1994) 1394.

9. VV. Shepelevich, S.F. Nichiporko, A.E. Zagaorskiy, Yi Hu, and A.A. Firsov, *Ferrolectrics* **266** (2002) 305.

10. B. I. Sturman *et al.*, *Phys. Rev. E* **60** (1999) 3332.

11. N.V. Kukhtarev, G.E. Dovgalenko, and V.N. Starkov, *Appl. Phys. A* **33** (1984) 227.

12. N.V. Kukhtarev, T.V.Kuktareva, J. Jones, E. Ward, and H.J. Caulfield, *Opt.Comm.* **104** (1993) 23.

13. J.G. Murillo, L.F. Magaña, M. Carrascosa, and F. Agulló-López, *J. Opt. Soc. Am. B* **15** (1998) 2092.

14. J.G. Murillo, L.F. Magaña, M. Carrascosa, and F. Agulló-López, *J. Appl. Phys.* **78** (1995) 5686.

15. R.V. Litvinov and S.M. Sandarov, *Quantum Electron* **11** (2001) 973.

16. C.L. Woods, C.L. Matson, and M.M. Salour, *Appl. Phys. A* **40** (1986) 177.

17. J.P. Herriau, D. Rojas, and J.P. Huignard, *Ferroelectrics* **75** (1987) 271.